RAPID COMMUNICATIONS

PHYSICAL REVIEW A VOLUME 42, NUMBER 1 1 JULY 1990

Modulational instability for normal dispersion

Joshua E. Rothenberg
IBM Thomas J. Watson Research Center, P.O. Box 218, Yorktown Heights, New York 10598
(Received 5 January 1990)

The observation of modulational instability of optical waves in the normal dispersion region has been accomplished through the copropagation of two nonlinearly coupled, orthogonally polarized visible waves in a strongly birefringent optical fiber. Intensity autocorrelations exhibit ~3.5-THz oscillations on both waves, and each wave spectrum develops a single shifted frequency sideband. The results agree well with an analysis of coupled nonlinear Schrödinger equations.

Modulational instability (MI) is a ubiquitous phenomenon, first studied some 20 years ago in the context of water waves,[1,2] and it is exhibited in many nonlinear wave systems.[1-11] MI is characterized by the instability of continuous waves to amplitude perturbations of certain frequencies, which grow exponentially. MI has been shown to be closely related to the recurrence problem of Fermi, Pasta, and Ulam,[3,4] and to soliton formation.[5-7] The possibility of MI for nonlinear optical propagation was first suggested by Ostrovskii,[8] and is the temporal analog of the spatial instability in optical filamentation.[5] Optical MI was later analyzed in detail,[9] and it was pointed out that the effect would only be seen for anomalous group-velocity dispersion (GVD, $\partial^2 k/\partial\omega^2 < 0$), which occurs in glasses for $\lambda \gtrsim 1.3$ μm. This effect was first observed in the nonlinear propagation of infrared light in optical fibers.[10] The observation was characterized by high-frequency intensity modulation and the development of sidebands around the pump up and down shifted by the modulation frequency. Since the nonlinear propagation of coupled polarized light waves was analyzed,[11] it has been known that the nonlinear coupling of two continuous waves can extend the domain of instability of a single wave. In Ref. 11 it was shown that incoherently coupled nonlinear Schrödinger equations (NLSE's) can exhibit MI even for parametric regions where a single NLSE would be stable to modulation (i.e., for normal dispersion). MI of coupled waves has since been discussed for many physical systems.[12-18] Recently, incoherently coupled NLSE's were used to analyze MI for two orthogonally polarized waves, nonlinearly coupled by cross-phase modulation (XPM), copropagating in a birefringent optical fiber in the anomalous dispersion region.[15] The case of nonlinear coupling of optical waves of different frequencies was subsequently studied using a similar analysis and shown to exhibit MI for normal dispersion,[16] however, the necessary inclusion of coherent coupling terms in the NLSE's tends to inhibit MI in this case.[17] The system of Ref. 15, however, does not suffer from this difficulty, and I show in an extension of the analyses of Refs. 15 and 16 that MI can occur for normal dispersion when polarized waves are coupled in a birefringent fiber. MI has also been predicted for coupled orthogonally polarized waves in a birefringent medium where large wave intensities produce nonlinear index changes on the order of the linear birefringence.[18] Experimentally, there have been numerous recent observations of single-wave MI for anomalous GVD.[19-21] There was also a recent observation of MI for anomalous dispersion, where the MI was assisted by XPM by a visible wave.[22] In this case, however, the anomalous wave would experience MI at higher power without the second wave, and the symmetric sideband spectra of the anomalous wave were similar to that found for single-wave MI.

In this paper, by copropagating orthogonally polarized waves in a strongly birefringent fiber, temporal intensity self-oscillation caused by MI is observed in the normal dispersion region. The intensity autocorrelations of the output waves exhibit ~3.5-THz oscillations with 100% modulation depth. The spectrum of each wave shows the exponential buildup from threshold of a single sideband shifted by the modulation frequency, in contrast to the symmetric spectra observed in single-wave MI.[10]

Copropagating orthogonally polarized fields

$$\mathcal{E}_j(z,t) = \mathrm{Re}[E_j(z,t)e^{-i(\omega_0 t - k_j z)}]$$

in a strongly birefringent fiber are described accurately by a pair of coupled NLSE's,

$$\frac{\partial E_j}{\partial z} + \delta_j \frac{\partial E_j}{\partial t} + i\frac{b}{2}\frac{\partial^2 E_j}{\partial t^2} = in_2 k_0 \left(|E_j|^2 + \tfrac{2}{3}|E_{3-j}|^2 \right) E_j , \quad (1)$$

for $j=1$ and 2, where $k_0 = \omega_0/c$, $b = d^2k/d\omega^2$ is the dispersion, $\delta_1 = +\delta/2$, $\delta_2 = -\delta/2$, $\delta = v_{g_2}^{-1} - v_{g_1}^{-1}$ is the group-velocity mismatch of the two polarization modes, the time frame is chosen to travel with the average velocity $v_{g_{av}}^{-1} = (v_{g_1}^{-1} + v_{g_2}^{-1})/2$, and n_2 is the nonlinear index (Kerr) coefficient. This description ignores coherent coupling terms which, for large birefringence, have large-phase mismatch and can be neglected, provided the nonlinear birefringence is small compared to the static birefringence (here it is smaller by a factor of ~1000). Following Refs. 15 and 16, one notes that Eq. (1) have the continuous-wave solutions $E_j = A_j \exp(i\phi_j)$, where $\phi_j = n_2 k_0 (|A_j|^2 + \frac{2}{3}|A_{3-j}|^2)$, for $j=1$ and 2. Linear stability is evaluated by substituting $E_j = (A_j + u_j) \times \exp(i\phi_j)$ into Eq. (1). One keeps only linear terms in u_j and uses the ansatz $u_j = (r_j + is_j)\exp[i(Kz - \Omega t)]$. The algebra is simplified by assuming $|A_1|^2 = |A_2|^2 = P$, then

one obtains the dispersion relation

$$[(K-\kappa)^2-B][(K+\kappa)^2-B]=C^2, \quad (2)$$

where $\kappa=\delta\Omega/2$, $B=b\Omega^2(k_0n_2P+b\Omega^2/4)$, and $C=\frac{2}{3}k_0n_2Pb\Omega^2$. Equation (2) has the solutions

$$K^2=B+\kappa^2\pm[(B+\kappa^2)^2+C^2-(B-\kappa^2)^2]^{1/2}. \quad (3)$$

Instability is present when complex solutions exist for K. For normal GVD, b, B, and C are positive, and instability occurs only if $C>|B-\kappa^2|$. The power gain for the instability $2\,\mathrm{Im}(K)$ is plotted in Fig. 1 using the present experimental parameters $n_2=3.2\times10^{-16}$ cm/W, $\delta=1.6$ ps/m, $b=0.065$ ps^2/m, effective fiber core area 1.3×10^{-7} cm^2, and wavelength 600 nm. At low power the peak gain is found in a narrow band of frequencies near $\Omega_{max}\cong\delta/b$. Changing the birefringence (i.e., δ) thus provides a simple method of tuning the modulation frequency. As the power increases the gain bandwidth increases and shifts to lower frequency. For intensity greater than a critical value,

$$P_{critical}=3\delta^2/4bk_0n_2, \quad (4)$$

the gain ceases [Fig. 1(b)]. These characteristics are in contrast to single-wave MI, where $\Omega_{max}\sim\sqrt{P}$, and the peak gain increases linearly with power. It has been noted previously that single-wave MI can be thought of in terms of four-wave mixing[9] (FWM). The same is true in the two-wave MI described here. In the case of MI of a single wave in the anomalous dispersion region, nonlinear phase shifts[23] ($\sim n_2k_0P$), owing to the intensity dependence of the index, can phase match the FWM process. For normal GVD, however, the nonlinear phase shifts actually increase the phase mismatch, and therefore single-wave MI is not observed for normal GVD. In the present system, however, the birefringence of the fiber allows for the phase matching, as has been previously predicted and observed.[24-27] The nonlinear phaseshifts still increase the FWM phase mismatch, which explains the critical power phenomena noted in Eq. (4), i.e., for large enough powers the phase mismatch induced by nonlinear phaseshifts becomes so large that no gain exists at any frequency. Numerical solutions of Eq. (1) show that the slow wave develops a single sideband downshifted by Ω_{max} and the fast wave upshifted by Ω_{max}. This can also be understood from the phasematching condition $\Delta k_{fast}+\Delta k_{slow}=0$, where Δk is the wave-number shift of each sideband. Using the dispersion relations

$$k_j=k_{0j}+[v_{g_{av}}^{-1}\pm(\delta/2)]\Omega+(b/2)\Omega^2,$$

one obtains the condition $\Omega(b\Omega-\delta)=0$, when the fast wave is upshifted and the slow wave downshifted by Ω. Thus, one finds that, for low power, $\Omega_{max}\cong\delta/b$, and the sidebands shift so that they have approximately the same group velocity as the opposing pump wave. Again, the behavior of the coupled-wave MI contrasts to single-wave MI, where the pump develops symmetric up and down shifted sidebands.[10]

The experimental configuration used is shown in Fig. 2. A synchronously pumped, cavity dumped dye laser supplies 600-nm, 9-psec pulses at a repetition rate of 4 MHz. A polarizing Michelson interferometer produces a pair of orthogonally polarized pulses of equal intensity with a selected relative time delay. The combination of the polarizing beam splitter (PBS) and two $\lambda/4$ wave plates in the interferometer prevents reflection back towards the laser. The pulse pair is focused into an 18-m birefringent fiber (beat length of 1.3 mm, group-velocity mismatch of 1.6 ps/m, and core diameter of 4 μm), with its axes aligned to the polarizations of the input pulses. The output wave is selected at the fiber output by a polarizer (typical extinction of the opposite wave is 500:1), and is either autocorrelated or measured with a spectrometer. The autocorrelator uses a noncollinear, background-free arrangement with a 0.3 mm potassium dihydrogen phosphate crystal for second harmonic generation. Either measurement is made with a slow scan ($\sim$100 sec) and thus represents the average over many laser pulses. For all the data presented, the fast pulse trails the slow pulse by 25 psec at the input, so that the fast pulse, advancing $1.6\times18=29$ psec during propagation, has passed through the slow pulse and leads by 4 psec at the fiber output. Note that a single pulse, owing to its own nonlinear propa-

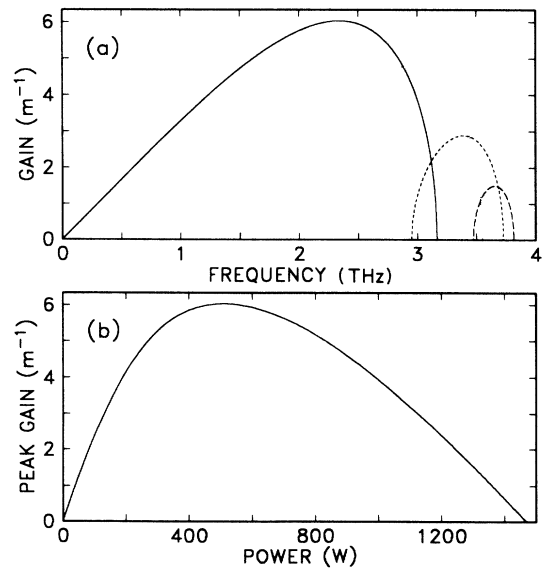

FIG. 1. (a) Calculation of MI gain vs frequency for group-velocity mismatch of 1.6 ps/m. Curves are (largest to smallest) for cw powers of 500, 250, 125, and 60 W. (b) MI peak gain vs power.

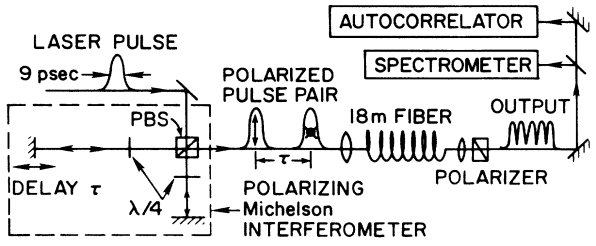

FIG. 2. Apparatus used to observe MI. PBS creates a pair of polarized pulses which are aligned with the axes of the birefringent fiber.

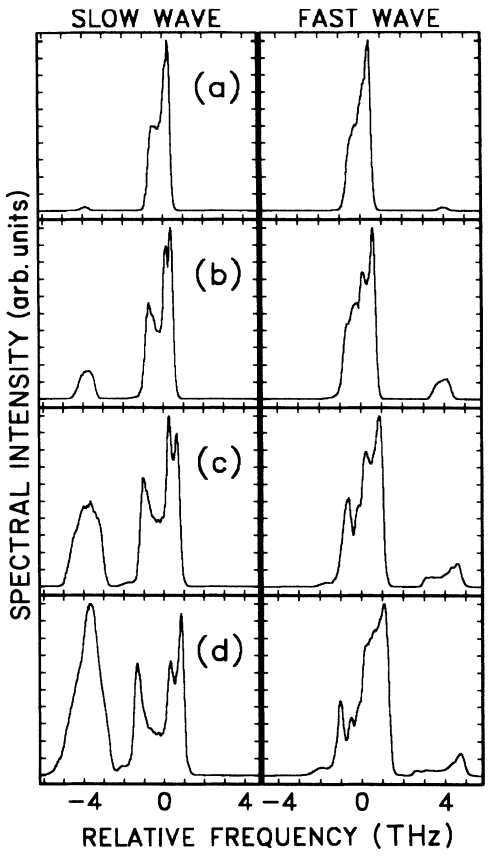

FIG. 3. Measurements of the spectra of the fiber output for the slow (first) and fast waves (second column) at peak input powers of (a) 90, (b) 110, (c) 170, and (d) 220 W. Zero frequency corresponds to the frequency of the input pulses.

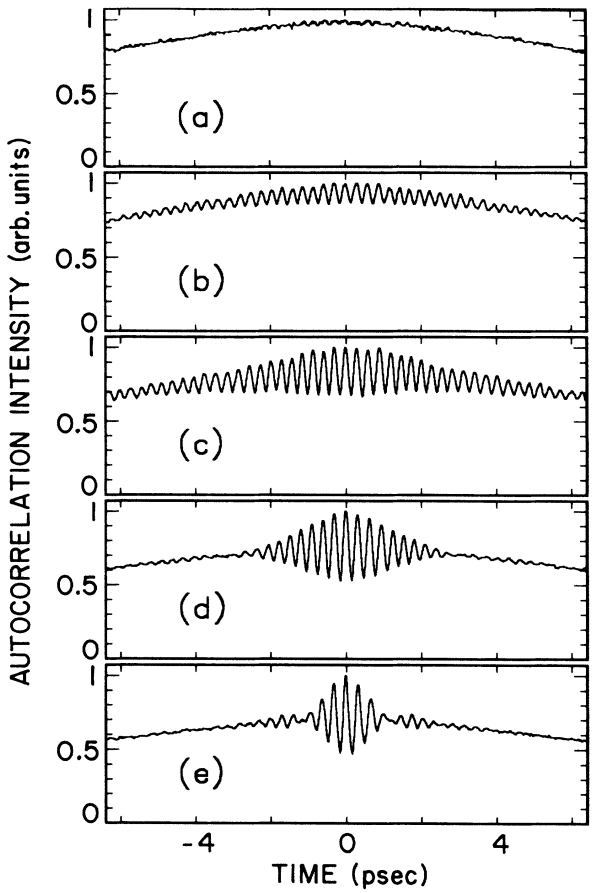

FIG. 4. Background-free autocorrelations of the slow output wave for peak input powers of (a) 90, (b) 110, (c) 140, (d) 170, and (e) 220 W. The intensity baseline is the true zero.

gation will broaden to 15–20 psec for peak input powers of 100–250 W. Thus the pulses only begin to overlap after ~8 m of propagation.

Figure 3 shows the spectra of the fiber output for the slow (first) and fast (second column) waves at a series of power levels near and above threshold. In Fig. 3(a), with the peak input power of both pulses set to 90 W, one sees just the slight appearance of a single sideband on each wave. Although the pump has broadened significantly from self-phase modulation, the generated single sideband is clearly resolved on each wave. The fast-wave sideband is upshifted and the slow-wave sideband is downshifted as predicted by the theory. In Fig. 3(b) where the power has been increased by only 20% to 110 W, one sees a sevenfold increase in the sideband power, demonstrating the threshold nature of the MI process. Given an amplification threshold of ~exp(16) and the effective interaction length of 8 m, one predicts a gain threshold of $2m^{-1}$, which is in agreement with the calculated peak gain from Fig. 1. As the power is increased beyond threshold [Figs. 3(c) and 3(d)], the sideband on the slow wave grows rapidly and severely depletes the pump, whereas the sideband on the fast wave saturates at a low power. This extreme asymmetry between the Stokes and anti-Stokes sidebands has been noted before as an important effect in four-wave mixing, and is understood to be the result of Raman gain and absorption for the Stokes and anti-Stokes bands, respectively.[26,27]

Figure 4 shows autocorrelations of the slow wave for increasing powers. At threshold in Fig. 4(a) one can possibly see the slight appearance of intensity oscillations. Just above threshold [Fig. 4(b)] there are very uniform oscillations at a frequency of 3.6 THz. The uniformity of the oscillations is somewhat surprising, given that the pump and stokes wave have THz spectral breadth. One therefore sees that, although generated over a broad bandwidth, the frequencies are phased in such a way as to produce uniform modulation. As the power is increased the frequency decreases to ~3.0 THz in Fig. 4(e), in good agreement with the calculation of Fig. 1. The fast wave shows similar behavior except that at higher powers the depth of modulation decreases because of Raman absorption of the anti-Stokes sideband. Note that the autocorrelation of a uniform 100% modulated sinusoid would have a peak to minimum ratio of 3:1. The observed ratio in Fig. 4 nears this value [2.2:1 in Fig. 4(e)], and given the large variation in the amplitude of the oscillations it appears the peak modulation depth approaches 100%. An interesting feature in the data is that the *envelope* of the oscillations becomes narrower and at the highest powers develops oscillatory structure. The narrowing of the envelope may be understood as partly because of the increased bandwidth

(see Fig. 1) at higher powers. For example, from Fig. 1 one calculates an effective MI bandwidth of ~ 0.3 THz at 170 W, which corresponds to an envelope width of ~ 2 psec [Fig. 4(d)]. The oscillatory envelope structure in the autocorrelation at higher powers would appear to indicate similar structure in the wave intensity, and may be related to the complicating effects of self-phase modulation of the input pulses, pump depletion, and/or Raman scattering.[28] Finally, it is interesting to note that this type of complicated behavior is similar to that found in other nonlinear wave systems,[4,6,28] and has been suggested to be related to nonlinear recurrence.[3,4,6,29]

[1]G. B. Whitham, J. Fluid Mech. **27**, 399 (1967).
[2]T. B. Benjamin and J. E. Feir, J. Fluid Mech. **27**, 417 (1967).
[3]E. Fermi, J. Pasta, and S. Ulam, in *Collected Papers of Enrico Fermi,* edited by E. Segre (University of Chicago, Chicago, 1965), Vol. 2, p. 978.
[4]H. C. Yuen and W. E. Ferguson, Phys. Fluids **21**, 1275 (1978).
[5]V. I. Bespalov and V. I. Talanov, Pis'ma Zh. Eksp. Teor. Fiz. **3**, 471 (1966) [JETP Lett. **3**, 307 (1966)].
[6]H. Hasimoto and H. Ono, J. Phys. Soc. Jpn. **33**, 805 (1972).
[7]A. Hasegawa, Opt. Lett. **9**, 288 (1984).
[8]L. A. Ostrovskii, Zh. Eksp. Teor. Fiz. **51**, 1189 (1966) [Sov. Phys. JETP **24**, 797 (1967)].
[9]A. Hasegawa and W. F. Brinkman, IEEE J. Quant. Elect. **QE-16**, 694 (1980).
[10]K. Tai, A. Hasegawa, and A. Tomita, Phys. Rev. Lett. **56**, 135 (1986).
[11]A. L. Berkhoer and V. E. Zakharov, Zh. Eksp. Teor. Fiz. **58**, 903 (1970) [Sov. Phys. JETP **31**, 486 (1970)].
[12]G. J. Roskes, Stud. Appl. Math. **55**, 231 (1976).
[13]K. P. Das and S. Sihi, J. Plasma Phys. **21**, 183 (1979).
[14]C. J. McKinstrie and R. Bingham, Phys. Fluids B **1**, 230 (1989).
[15]C. R. Menyuk, IEEE J. Quant. Elect. **QE-23**, 174 (1987).
[16]G. P. Agrawal, Phys. Rev. Lett. **59**, 880 (1987).
[17]J. E. Rothenberg, Phys. Rev. Lett. **64**, 813 (1990).
[18]S. Wabnitz, Phys. Rev. A **38**, 2018 (1988).
[19]K. Tai, A. Tomita, J. L. Jewell, and A. Hasegawa, Appl. Phys. Lett. **49**, 236 (1986).
[20]M. Nakazawa, K. Suzuki, and H. A. Haus, Phys. Rev. A **38**, 5193 (1988).
[21]M. Nakazawa, K. Suzuki, and H. A. Haus, IEEE J. Quant. Elect. **QE-25**, 2036 (1989).
[22]A. S. Gouveia-Neto, M. E. Faldon, A. S. B. Sombra, P. G. J. Wigley, and J. R. Taylor, Opt. Lett. **13**, 901 (1988).
[23]R. S. Stolen and J. E. Bjorkholm, IEEE J. Quant. Elect. **QE-18**, 1062 (1982).
[24]R. S. Stolen, M. A. Bosch, and C. Lin, Opt. Lett. **6**, 213 (1981).
[25]R. K. Jain and K. Stenersen, Appl. Phys. B **35**, 49 (1984).
[26]R. S. Stolen, IEEE J. Quant. Elect. **QE-11**, 100 (1975).
[27]K. Stenersen and R. K. Jain, Opt. Commun. **51**, 121 (1984).
[28]A. S. Gouveia-Neto, M. E. Faldon, and J. R. Taylor, Opt. Lett. **13**, 1029 (1988).
[29]N. J. Zabusky and M. D. Kruskal, Phys. Rev. Lett. **15**, 240 (1965).